Two-phase mixture model for nanofluid turbulent flow and heat transfer: Effect of heterogeneous distribution of nanoparticles

CrossMark

Mohammad Amani [a], Pouria Amani [b], Alibakhsh Kasaeian [c], Omid Mahian [d,*], Wei-Mon Yan [e]

[a] *Mechanical and Energy Engineering Department, Shahid Beheshti University, Tehran, Iran*
[b] *Department of Chemical Engineering, Faculty of Engineering, University of Tehran, Tehran, Iran*
[c] *Department of Renewable Energies Engineering, Faculty of New Sciences & Technologies, University of Tehran, Tehran, Iran*
[d] *Renewable Energies, Magnetism and Nanotechnology Lab., Faculty of Science, Ferdowsi University of Mashhad, Mashhad, Iran*
[e] *Department of Refrigerating Air-Conditioning Engineering, National Taipei University of Technology, Taipei 10608, Taiwan*

HIGHLIGHTS

- Two-phase mixture model of SiO_2/water nanofluids in turbulent flow is proposed.
- Heterogeneity of concentration due to crossed effect and Brownian motion are considered.
- Considering heterogeneous concentration gives more close results to experimental data.

ARTICLE INFO

ABSTRACT

In this work, a two-phase mixture model for evaluation of flow and heat transfer performance of SiO_2/water nanofluids under turbulent flow was proposed by considering the heterogeneity of concentration due to crossed effect and the influences of shear rate, viscosity gradient, thermophoresis and Brownian motion on the diffusion of the nanoparticles. The effects of Peclet number, Reynolds number, nanoparticle size and nanofluid mean concentration on the distribution of nanoparticles have been evaluated. The values of thermal conductivity and viscosity as the main thermophysical properties of nanofluids changed across different layers of the liquid due to the heterogeneous distribution of concentration. It was observed that an increase in the Peclet number caused heterogeneity in the distribution of the properties. The achieved nanoparticle distribution has been implemented for analysis of nanofluid using two-phase mixture model. It was found that the effect of nanofluid concentration on the Nusselt number was more noticeable in lower Reynolds numbers due to the insignificant effect of flow momentum on heat transfer. The maximum of 43.9% enhancement in convection heat transfer was achieved by dispersion of 4% SiO_2 nanoparticles inside DI-water at *Re* = 25,000.

© 2017 Elsevier Ltd. All rights reserved.

1. Introduction

Suspensions containing nanoparticles with a size of 1–100 nm have wide applicability in heating and cooling industries. During last decade, many researchers have evaluated the properties and influence of nanofluids on the heat transfer improvement in thermal systems, for example see Refs. (Colangelo et al., 2015; Milanese et al., 2016a, 2016b; Colangelo et al., 2016a, 2016b; Milanese et al., 2016; Iacobazzi et al., 2016; Amani et al., 2017a, 2017b, 2017c; Lomascolo et al., 2015; Cai et al., 2017). Flow-induced particle migration is an essential mechanism in suspension rheology in various engineering applications such as sequestration processes in porous media, chromatography, heat transfer, oil recovery, transport of sediments and composite materials, which can considerably enhance the heat transfer rate in nanofluids by modifying the thermophysical properties and intensifying the heterogeneity of concentration distribution. The homogeneous models presented for nanofluid do not consider all fluid-particle interactions in the hydrothermal analysis. Therefore, it is essential to model the nanofluid as a heterogeneous two-phase mixture and physically consider the particle movements to successfully predict the dynamics of nanoparticles as well as the mechanism of thermal transport in nanofluids.

* Corresponding author.
E-mail addresses: m_amani@sbu.ac.ir (M. Amani), pouria.amani@ut.ac.ir (P. Amani), akasa@ut.ac.ir (A. Kasaeian), omid.mahian@gmail.com (O. Mahian), wmyan1234@gmail.com (W.-M. Yan).

Nomenclature

A	area (m^2)		μ	dynamic viscosity (Pa s)
d_p	particle diameter (m)		λ	thermal conductivity (W/m K)
D_T	thermophoresis coefficient		$\dot{\gamma}$	shear rate (1/s)
D_B	Brownian diffusion coefficient		κ	turbulent kinetic energy
g	gravitational acceleration (m^2/s)		ε	rate of dissipation
G_κ	generation of turbulence kinetic		σ_ε	effective Prandtl numbers for turbulent kinetic energy
J	total flux of particle migration (kg/m^2 s)		σ_κ	effective Prandtl numbers for rate of dissipation
K_c, K_μ	phenomenological constants		μ_t	eddy viscosity (Pa s)
k_B	Boltzmann's constant		η	thermal performance index
Nu	Nusselt number			
P	pressure (Pa)		*Subscripts*	
Pe	Peclet number		atm	atmosphere
q''	heat flux (w/m^2)		B	thermophoresis
r	radial coordinate (m)		dr	drift
Re	Reynolds number		f	base fluid
T	Temperature (K)		m	mixture
u	axial velocity (m/s)		nf	nanofluid
V	velocity (m/s)		p	particle
$\bar{V}$	time-averaged fluid velocity (m/s)		S	non-homogenous shear rate
x	longitudinal component (m)		T	thermophoresis
			μ	viscosity gradient
Greek letters				
φ	nanoparticle fraction			
ρ	density (kg/m^3)			

Lam et al. (2004) studied the poiseuille flow of shear-induced particle migration of micron-sized particles suspended in a base fluid. They observed that the shear-thinning of base fluid could improve particle migration from the higher shear rate region toward the lower shear rate region. Therefore, the minimum particle concentration was obtained adjacent to tube surface and rapidly increased up to radius ratio of 0.8–0.9 corresponding the maximum particle concentration and starts to decline to the center of the tube. Chen et al. (2004) investigated the shear-induced particle migration in a concentrated suspension using a phenomenological diffusive flux model. They revealed that particle migration plays a pivotal role to determine the flow pattern of concentrated suspensions.

Nanofluids flowing through the tubes lead to increase the heat transfer in conventional heat exchangers and heating/cooling units. This significant improvement of heat transfer is the reason of great usage of the nanofluids in the last decade. By reviewing the published studies, it is revealed that molecular-level layering of the liquid at the particle-liquid interface (Keblinski et al., 2002), energy transfer by nanoparticle dispersion (Xuan and Roetzel, 2000; Xuan and Li, 2003), increased thermal conductivity (Kasaeian et al., 2015; Raja et al., 2016) as well as Brownian motion and thermophoresis diffusion (Yang et al., 2016) have been introduced as possible reasons behind the heat transfer improvement of nanofluids. A few studies have been conducted on the effect of nanoparticle migration on heat transfer characteristics of nanofluids. Here, some of these studies are reviewed briefly. Wen and Ding (2004) studied the nanoparticle migration in laminar flow in a tube and observed that the nanoparticle concentration is smaller near the tube surface in comparison with the center of the tube. Bahiraei and Hosseinalipour (2013) studied the influence of particle migration on TiO$_2$ nanoparticle distribution and laminar convection heat transfer considering thermophoresis in a tube by using dispersion model. Their results showed that thermophoresis played a substantial role in the particle migration. Thermophoresis caused the velocity profile flatter and the concentration more non-uniform. Moreover, greater convection heat transfer coefficient

was achieved by considering thermophoresis in all Reynolds numbers in their study. Later, Bahiraei (2016) presented a comprehensive review of investigations conducted on particle migration in nanofluids including Eulerian-Lagrangian, molecular dynamics, and Buongiorno methods. The author concluded that the results of different research groups are inconsistent.

There are two different approaches in the literature for modeling the flow and heat transfer of nanofluid i.e. single-phase and two-phase methods. In single-phase method, nanofluids are assumed as homogeneous fluids considering zero relative velocity and thermal equilibrium of liquid and solid phases. The numerical analysis using single-phase method is implemented by considering uniform particle distribution and the effective thermal conductivity, density, and viscosity of nanofluid. Some of the investigations show that the results of homogeneous assumption for nanofluids are very close to the experimental data since the nanoparticles are very tiny (Keshavarz Moraveji and Hejazian, 2012). On the other hand, some studies have implemented the two-phase method for modeling of nanofluid flow such as two-phase Euler-Lagrange model and mixture model. The former method considers the base fluid and nanoparticles as a continuous and dispersed phase, respectively. In this approach, the interaction between nanoparticles and base fluid and related forces are taken into account. The substantial issue in the mixture model is that just one setoff velocity component is solved for mixture momentum equation. In this model, the interaction between the primary and secondary phase occurs through drag, turbulence and reduction in momentum. Kakaç and Pramuanjaroenkij (2016a, 2016b) and Vanaki et al. (2016) summarized the numerical studies applying both single-phase and two-phase approaches to study the performance of nanofluids. Keshavarz Moraveji and Hejazian (2012) analyzed the turbulent forced convective heat transfer of Al$_2$O$_3$/water nanofluids in a tube using two-phase Euler-Lagrange and mixture models comparatively. According to their analysis, mixture model was more accurate than the other approach. Siavashi and Jamali (2016) conducted a numerical analysis of TiO$_2$/water nanofluid through annuli using two-phase mixture model in turbulent flow

regime. Their results showed a satisfactory agreement with the experimental data. Sert and Sezer-Uzol (2016) studied the fully developed laminar flow of nanofluids in a circular tube with two-phase mixture model. They revealed that two-phase approach gives higher heat transfer coefficients compared to single-phase modeling. Shariat et al. (2013) investigated the influence of nanofluid concentration on convective heat transfer in a horizontal elliptic duct employing two-phase mixture model. They observed that the thermal properties improve and pressure drop increases by an increment in nanoparticle concentration.

The nanoparticles distribute in the base fluid non-uniformly due to particle migration caused by shear-induced migration, Brownian motion, thermophoretic migration and viscosity gradient which affect the flow and heat transfer performance. Effective properties including thermal conductivity and viscosity have remarkable impact on convection heat transfer and pressure drop of nanofluids. Therefore, nanoparticle distribution inside the carrier liquid is critical in nanofluid analysis which has been neglected in the single-phase method.

There are a few studies in the literature concerning the hydrothermal analysis of nanofluid as a two-phase mixture incorporating non-uniform distribution of nanofluid concentration (Wen et al., 2009; Heyhat and Kowsary, 2010; Bahiraei, 2015). In these studies, the flow regime was assumed to be laminar. To the best knowledge of the authors, there is no published study considering the effect of the heterogeneous distribution of nanoparticles in turbulent fluid flow; so the scarcity of study in this subject is felt strongly. The aim of this article is to explore the nanoparticle distribution by employing two-phase mixture model which incorporates the effective parameters on particle migration including viscosity gradient-induced migration, non-homogenous shear rate, thermophoresis and Brownian motion. Indeed, the heterogeneity of nanoparticles concentration caused by crossed effect is considered in the model.

2. Mathematical modeling

In this numerical analysis, water-based SiO_2 nanofluids have been considered as the working fluid. The geometrical configuration consists of a tube with a length and a diameter of 1.0 m and 0.01 m, respectively, shown in Fig. 1. The flow has been considered to be fully developed both hydrothermally and thermally.

2.1. Nanoparticle distribution

Considering homogenous (single-phase) medium with a uniform distribution of nanoparticles may lead to significant errors in the prediction of nanofluid performance, especially at high concentrations. In fact, one of the main factors accounting for inconsistencies prevalent in nanofluid research projects is ignoring the effects of particle migration on flow and heat transfer characteristics. Taking into account the particle migration in modeling can modify the results since the distribution of particle concentration has been involved. Physically, the particle migration idea is to consider that nanofluids are a heterogeneous two-phase mixture. There are four mechanisms which have a significant impact on particle migration. Viscosity gradient causes nanoparticles to concentrate in lower viscosity regions, while shear rate makes the particles travel from higher shear region to lower one. Thermophoresis is particle motion induced by a temperature gradient, and Brownian motion compels particles to migrate from the area with high concentration to those with lower concentration. It is reported that thermophoresis can have stronger effects on particles compared to that of Brownian diffusion. The thermophoretic force exerts on the particles in the opposite direction of the temperature gradient. Moreover, this force makes the velocity profile flatter and raises the convective heat transfer coefficient which its effect is more pronounced at greater mean concentrations (Bahiraei, 2017).

Mass conservation for particle phase is presented in Eq. (1) for a fully developed flow of nanofluids in a horizontal tube with the steady-state condition (Ding and Wen, 2005).

$$J + r\frac{dJ}{dr} = 0 \tag{1}$$

where J and r are the total flux of particle migration and radial coordinate, respectively. As previously mentioned, the total flux of particles consists of four terms as below:

$$J = J_S + J_\mu + J_T + J_B \tag{2}$$

where J_S, J_μ, J_T and J_B represent the flux of particles associated with non-homogenous shear rate, viscosity gradient, thermophoresis and Brownian motion, respectively. These particle fluxes are proposed by Phillips et al. (1992) and Buongiorno (2006) as follows.

$$J_s = -K_c d_p^2(\varphi^2 \nabla\dot{\gamma} + \varphi\dot{\gamma}\nabla\varphi) \tag{3}$$

$$J_\mu = -K_\mu \dot{\gamma}\varphi^2\left(\frac{d_p^2}{\mu}\right)\frac{d\mu}{d\varphi}\nabla\varphi \tag{4}$$

$$J_t = -D_T\frac{\nabla T}{T} \tag{5}$$

$$J_B = -D_B\nabla\varphi \tag{6}$$

where K_c and K_μ represent phenomenological constants, μ denotes viscosity, d_p denotes the particle diameter, φ accounts for the concentration, and $\dot{\gamma}$ is the shear rate. In addition, D_T and D_B are thermophoresis and Brownian diffusion coefficients, respectively, which can be calculated as follows (Russell et al., 1991; McNab and Meisen, 1973).

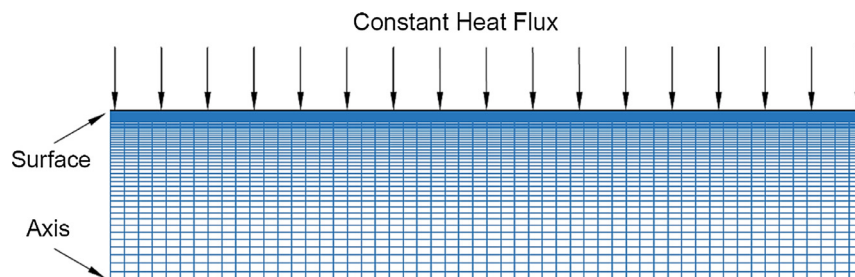$$D_T = \left(0.26\frac{\lambda}{2\lambda + \lambda_p}\right)\frac{\mu}{\rho}\varphi \tag{7}$$

Fig. 1. Two-dimensional geometry of analysis.

$$D_B = \frac{k_B T}{3\pi\mu d_p} \tag{8}$$

where ρ denotes density, λ is thermal conductivity, and k_B and T represent Boltzmann's constant and the nanofluid temperature. Subscript p refers to nanoparticles.

By implementing symmetrical boundary condition at $r = 0$ and integrating Eq. (1), the following equation is derived.

$$J = J_S + J_\mu + J_T + J_B = 0 \tag{9}$$

By replacing the particle fluxes obtained from Eqs. (3)–(6) into Eq. (9), the following equation can be obtained:

$$K_c d_p^2 (\varphi^2 \nabla \dot\gamma + \varphi \dot\gamma \nabla \varphi) + K_\mu \dot\gamma \varphi^2 \left(\frac{d_p^2}{\mu}\right) \frac{d\mu}{d\varphi} \nabla \varphi + D_T \frac{\nabla T}{T} + D_B \nabla \varphi = 0 \tag{10}$$

Because the fluid is assumed Newtonian, we define the shear rate as follows.

$$\dot\gamma = \frac{1}{2\mu}\left(\frac{dP}{dx}\right)r \tag{11}$$

where P and x represent the pressure and longitudinal component, respectively.

To solve Eq. (10), the thermophoresis term should be stated concerning concentration. Also, viscosity and thermal conductivity correlations are demanded. For this purpose, the models proposed by Brinkman (1952) and Yu and Choi (2003) are implemented as follows.

$$\mu = \frac{1}{(1-\varphi)^{2.5}}\mu_f \tag{12}$$

$$\lambda = \lambda_f \left[\frac{2\lambda_f + \lambda_p + 2(\lambda_p - \lambda_f)(1+\beta)^3 \varphi}{2\lambda_f + \lambda_p - (\lambda_p - \lambda_f)(1+\beta)^3 \varphi}\right] \tag{13}$$

where β is assumed to be 0.1 (Yu and Choi, 2003).

The boundary condition which is required for solving Eq. (10) is:

$$\varphi_m = \frac{\int \varphi(r)dA}{\int dA} \tag{14}$$

where φ_m and A represent the mean concentration and area, respectively.

The Peclet number is expressed as:

$$Pe = \frac{3\pi d_p^3 (-dP/dx)R}{2k_B T} \tag{15}$$

The Peclet number can be defined as the ratio of particle migration induced by convection to particle migration induced by Brownian motion. In fact, shear rate directs the particles into the lower shear region; Brownian motion moves the particles into the less-concentrated regions. In other words, Brownian motion and shear rate respectively lead to uniformly concentration distribution and inversely heterogeneous distribution. Thus, the smaller Peclet number leads to remarkable effects of Brownian motion on particles migration.

The concentration distribution of SiO_2 nanoparticles into the water in a fully-developed region of a tube is determined by solving Eq. (10). Accordingly, considering nanoparticles migration and the resultant heterogeneous concentration distributions and useful properties, which are the two-phase flow nature of nanofluids, is required to develop a proper modeling of the convective heat transfer of nanofluids.

2.2. Two-phase mixture model

The nanofluid flow is considered incompressible and steady-state, and the viscose dissipation is neglected. The equations of continuity, momentum, energy, and volume fraction of nanoparticles for two-phase mixture model can be expressed as follows.

Continuity equation:

$$\nabla \cdot (\rho_m V_m) = 0 \tag{16}$$

Momentum equation:

$$\nabla \cdot (\rho_m V_m V_m) = -\nabla P + \nabla \cdot (\mu_m (\nabla \cdot V_m + \nabla \cdot V_m^T)) + \nabla \\ \cdot \left(\sum_k \varphi_k \rho_k V_{dr,k} V_{dr,k}\right) \tag{17}$$

Energy equation:

$$\nabla \cdot \sum_k \varphi_k V_k \rho_k C_{p,k} T = \nabla \cdot (\lambda_m \nabla T) \tag{18}$$

Volume fraction of nanoparticles:

$$\nabla \cdot (\varphi_p \rho_p V_m) = -\nabla \cdot (\varphi_p \rho_p V_{dr,p}) \tag{19}$$

where V denotes velocity and φ_k and $V_{dr,k}$ represent the volume fraction and drift velocity of phase k. The subscripts p, f, and m represent nanoparticles, base fluid and mixture, respectively. The mixture density, viscosity, thermal conductivity, mass average velocity along with the drift velocity of nanoparticles are defined as following.

$$\rho_m = \sum_k \varphi_k \rho_k \tag{20}$$

$$\mu_m = \sum_k \varphi_k \mu_k \tag{21}$$

$$\lambda_m = \sum_k \varphi_k \lambda_k \tag{22}$$

$$V_m = \frac{\sum_k \varphi_k \rho_k V_k}{\rho_m} \tag{23}$$

$$V_{dr,k} = V_k - V_m \tag{24}$$

The relative velocity of between nanoparticle and base fluid which is proposed by Manninen et al. (1996) is presented in Eq. (25).

$$V_{pf} = V_p - V_f = \frac{\rho_p d_p^2}{18\mu_f f_{drag}} \frac{(\rho_p - \rho_m)}{\rho_p}(g - (V_m \cdot \nabla)V_m) \tag{25}$$

The drag function (i.e. f_{drag}) can be determined using Schiller and Naumann's correlation (Schiller and Naumann, 1935).

$$f_{drag} = \begin{cases} 1 + 0.15 Re_p^{0.687} & Re_p \leqslant 1000 \\ 0.0183 Re_p & Re_p > 1000 \end{cases} \tag{26}$$

It is noteworthy mentioning that these characteristics are functions of the mixture of the nanofluid and moreover, spatial-dependent due to the possible heterogeneity of nanoparticle concentration.

2.3. Turbulent modeling

In this numerical analysis, the κ-ε turbulent model is implemented. Moreover, turbulent kinetic energy (κ) and rate of dissipation (ε) equations are required to be solved, which are given as follows:

$$div(\rho\bar{V}\kappa) = div\left(\frac{\mu + \mu_t}{\sigma_\kappa \nabla \kappa}\right) + G_\kappa - \rho\varepsilon \qquad (27)$$

$$div(\rho\bar{V}\varepsilon) = div\left\{\left(\mu + \left(\frac{\mu_t}{\sigma_\varepsilon}\right)\right)\nabla\varepsilon\right\}C_{1\varepsilon}\left(\frac{\varepsilon}{\kappa}\right)G_\kappa + C_{2\varepsilon}\rho\left(\frac{\varepsilon^2}{\kappa}\right) \qquad (28)$$

where $\bar{V}$ represents the time-averaged fluid velocity and σ_ε, and σ_κ represent effective Prandtl numbers for the rate of dissipation and turbulent kinetic energy respectively. Also, G_κ denotes the generation of turbulent kinetic energy because of the mean velocity gradients, $C_{1\varepsilon}$ and $C_{2\varepsilon}$ are constant, and μ_t is eddy viscosity. In Eqs. (27) and (28): $C_{1\varepsilon}$ = 1.44, $C_{2\varepsilon}$ = 1.92, σ_ε = 1.3 and σ_κ = 1.0 (Launder and Spalding, 1972). The eddy viscosity has been modeled by:

$$\mu_t = \frac{(\rho C_\mu \kappa^2)}{\varepsilon} \qquad (29)$$

where C_μ is constant with a value of 0.09.

2.4. Boundary conditions

No-slip condition at the surface of the tube, a developed velocity and zero relative pressure (atmospheric static pressure) respectively at the inlet and outlet section of the tube, are specified as the flow boundary conditions. Moreover, the temperature at the inlet section was assumed to be uniform and a constant heat flux is imposed on the wall. Aminfar and Motallebzadeh (2012) reported that the influence of gravitational forces on the concentration distribution is insignificant in nanofluids. They observed that in both axial and radial directions, the velocity of the nanofluid slightly affects by particle motion due to gravitational and drag forces and is approximately has an order of 10^{-11}. Therefore, in this study, the influence of gravity on distribution is neglected which leads to no angle dependency in the equations. The mathematical form of boundary conditions are as:

– At the solid-fluid interface: u = 0, $-\lambda\partial T/\partial r = q''$.
– At the tube entrance (x = 0): $u = u_{const}$, T = 300 K.
– At the outlet section of the tube: $P = P_{atm}$.

3. Numerical method and validation

Control volume technique is used to discrete the set of equations. Furthermore, second order upwind method is employed to solve the momentum and energy equations, and velocity-pressure coupling is conducted using the SIMPLE approach. Finer meshes are used near the tube surface due to severe velocity, and temperature gradients exist there. Various numbers of meshes are evaluated to ensure grid independence, and as can be seen in Fig. 2, the mesh of 50 × 1300 nodes is selected as the proper mesh-

ing due to the observation of insignificant variation in the results of finer meshes.

For validation of numerical results and two-phase mixture model, the results of this analysis are compared with those calculated from the Gnielinski correlation (Gnielinski, 1976) in Eq. (30) for the Nusselt number, Blasius correlation (White and Corfield, 2006) in Eq. (31) for friction factor and experimental work of Sundar et al. (2012) for Fe_3O_4 nanofluid. These correlations are presented as below.

$$Nu = 0.012(Re^{0.87} - 280)Pr^{0.4}; 1.5 < Pr < 500, 3000 < Re < 10^6 \qquad (30)$$

$$f = 0.316Re^{-0.25}; 3000 < Re < 10^5 \qquad (31)$$

Fig. 3 confirms that the present results are in good agreement with presented correlations in the literature as well as experimental data of Sundar et al. (2012).

4. Results and discussion

The spatial-dependent concentration distribution in nanofluid occurs by particle migration, and subsequently, this distribution can affect the flow and heat transfer of the nanofluids. To study the non-linear effect of non-uniformity in concentration distribution on flow and convection heat transfer of SiO_2/water nanofluids, a numerical investigation is employed using two-phase mixture model.

Fig. 4 illustrates the distribution of nanoparticles at a cross section of the tube for mean concentrations of 1% and 4% with different Peclet numbers. It is clear that the heterogeneity of the concentration distribution enhances by the increment of Peclet
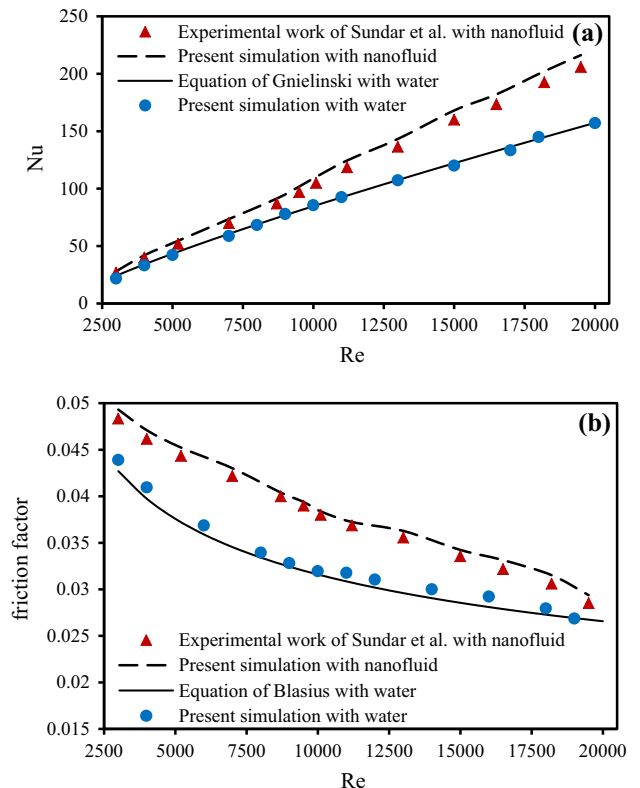

Fig. 2. Grid independency results.

Fig. 3. Validation of current analysis with Gnielinski and Blasius correlations (Gnielinski, 1976; White and Corfield, 2006) and experimental data of Sundar et al. (2012).
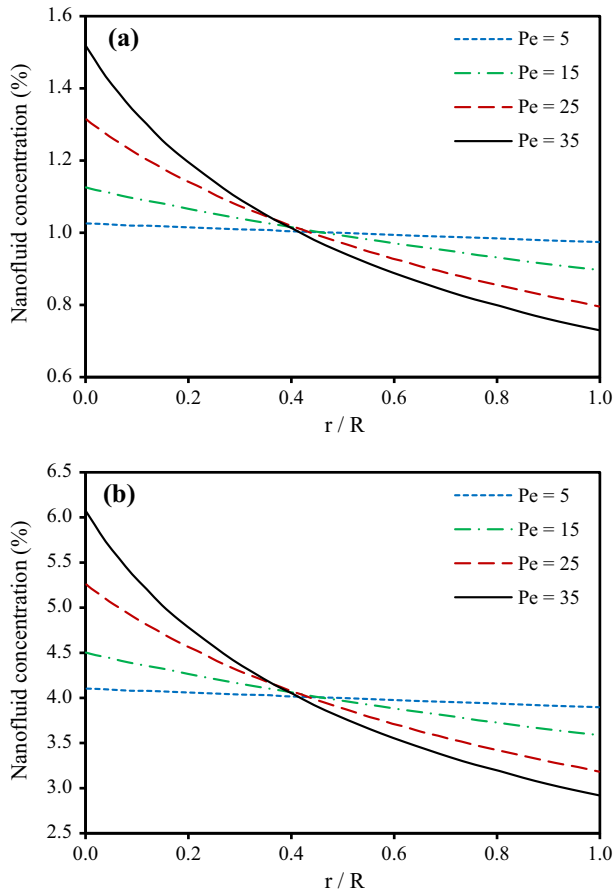
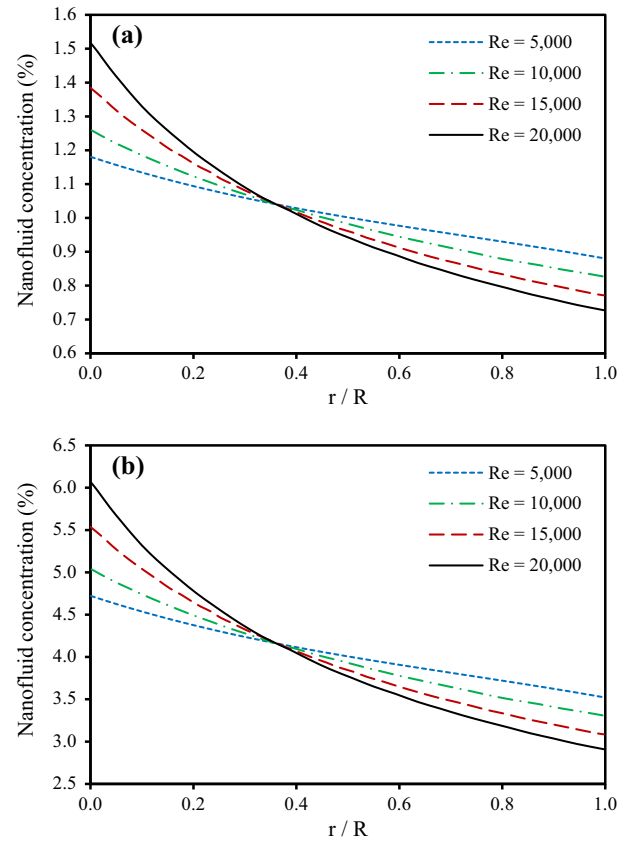Fig. 4. Nanofluid concentration distribution at various Peclet numbers for mean concentration of (a) 1% and (b) 4%.

Fig. 5. Nanofluid concentration distribution at different Reynolds numbers for mean concentrations of (a) 1% and (b) 4%.

number. For instance, the concentration increases from 2.92% near the tube surface to 6.07% at the center of the tube at $Pe = 35$ and $\varphi_m = 4\%$. As mentioned before, when the Peclet number increases, the contribution of Brownian motion is reduced compared to the other factors. On the other hand, the impact of Brownian motion will strengthen at low Peclet numbers and more homogeneous concentration distribution of nanoparticles is then achieved. Thus, at $Pe = 5$ and $\varphi_m = 4\%$, the concentration increases from 3.90% near the tube surface to 4.10% at the center of the tube.

Fig. 5 shows the concentration distribution for different Reynolds numbers at $\varphi_m = 1\%$ and 4% and $d_p = 50$ nm. It is seen that the increment of Reynolds number leads to non-uniform concentration distribution. With incrementing Reynolds number the pressure gradient increases in the nanofluid and according to Eq. (15), the Peclet number raises. Therefore, the effect of shear rate is more pronounced compared to Brownian motion in high Reynolds numbers and causes spatial heterogeneity in concentration distribution.

Fig. 6 depicts the effect of particle size on the concentration distribution at $Re = 20,000$ and $\varphi_m = 1\%$ and 4%. It is found that the finer particles distribute inside the base fluid more uniformly. The particle size has a direct impact on the particle fluxes which are associated with shear rate and viscosity gradient, while it has an opposite effect on Brownian motion. As can be seen, distribution of the particles is heterogeneous which the concentration is greater in central regions, and its heterogeneity intensifies with increasing the particle size. This heterogeneity is caused by factors which push the particles toward the center of the tube such as shear rate. Brownian motion of the particles is strongly dependent on their

size, and by reducing the size of particles, it intensifies significantly. The Brownian force is applied to the particles in the opposite direction of the concentration gradient. Thus, this force can push the particles from center to wall of the tube, and make the concentration more uniform. On the other hand, Peclet number magnitude is proportional with particle size with a power of three (d_p^3). Therefore, the enlargement of nanoparticles size remarkably increases the spatial heterogeneity of nanoparticles inside the base fluid. The distribution increases from 3.88% near to the tube surface to 4.07% at the center of the tube for $d_p = 10$ nm, while it changes from 2.74% to 6.72% for $d_p = 70$ nm at the mean concentration of 4%.

By decreasing the size of particles, the mean convective heat transfer coefficient increases. At a given concentration, the finer nanoparticles, the higher number of suspended particles in the base fluid, and higher Brownian motion. Also, with increasing the turbulence intensity inside the tube smaller particles are affected more, and therefore, random motion of particles becomes more intense, which can lead to the improvement of heat transfer rate. Moreover, by reducing the size of the particulate matter and consequently, intensification of the Brownian motion, the particles migrate more towards the channel walls, and therefore, the concentration of particles in the vicinity of the walls will increase, which in turn leads to increase in pressure drop.

The concentration distribution for various nanoparticle mean concentrations for $Re = 20,000$ and $d_p = 50$ nm is illustrated in Fig. 7. It is concluded that the non-uniformity of concentration distribution is increased by increasing the mean concentration. The concentration increases from 0.96% in the vicinity of tube surface to 1.06% at the center of the tube for $\varphi_m = 1\%$, while it is raised from 3.28% to 5.03% at $\varphi_m = 4\%$. According to Eqs. (3) and (4), the
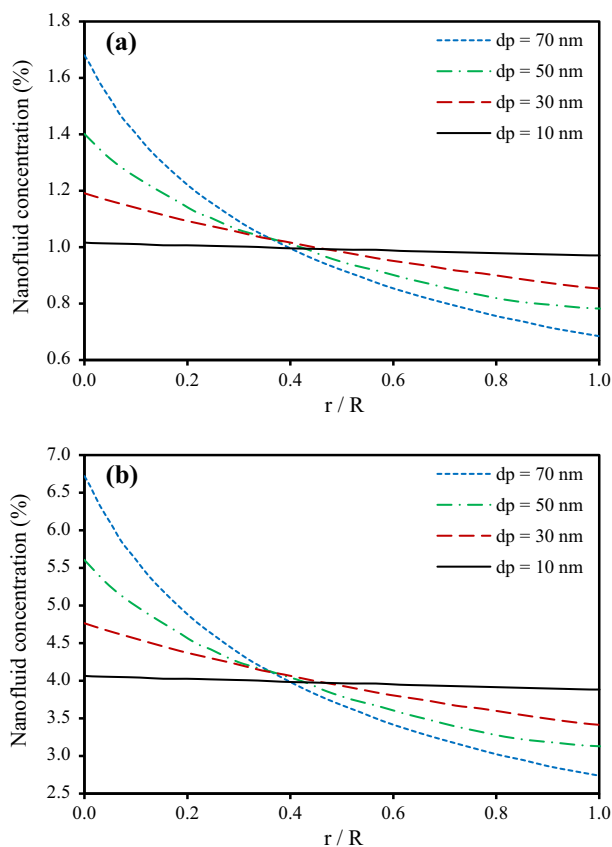
Fig. 6. Nanofluid concentration distribution at different sizes of nanoparticles for mean concentration of (a) 1% and (b) 4%.

Fig. 8. (a) Thermal conductivity (b) Viscosity distribution in the tube cross section for φ_m = 4% and d_p = 50 nm.
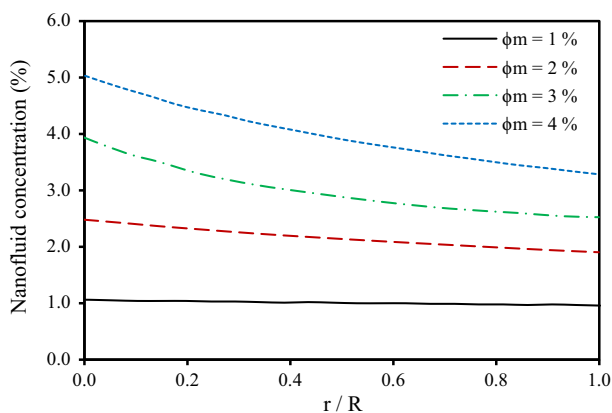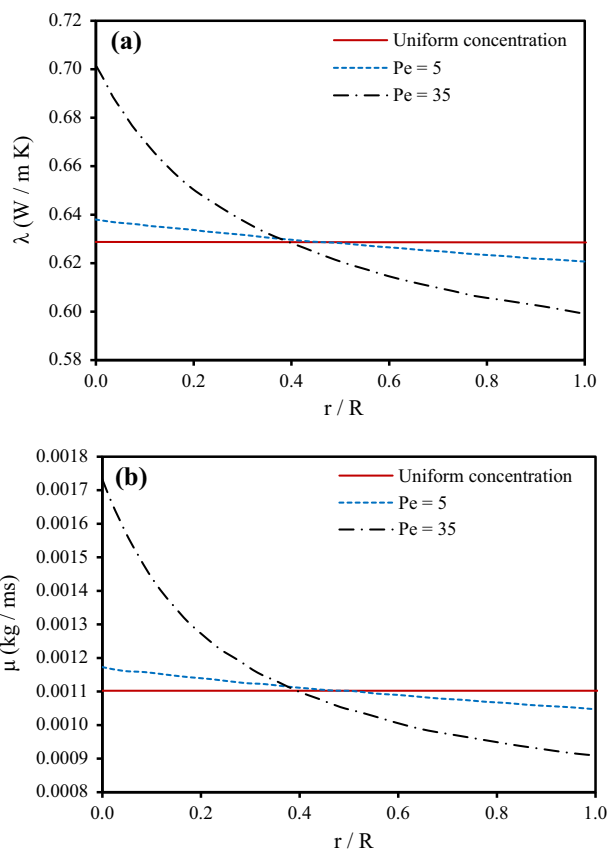

Fig. 7. Nanofluid concentration distribution at various mean concentrations for Re = 20,000.

concentration directly correlated to the particle fluxes related to shear rate and viscosity gradient, whereas based on Eq. (5), the concentration gradient is only proportional to the particle fluxes associated with Brownian motion.

Fig. 8 illustrates the thermal conductivity along with dynamic viscosity distribution of SiO$_2$/water nanofluids for φ_m = 4% and d_p = 50 nm at the tube cross section. It is seen that the increasing the Peclet number intensifies heterogeneity in the properties distribution. The thermal conductivity is raised from 0.599 W/mK near the tube surface to 0.701 W/mK at the center of the tube, whereas the viscosity varies from 0.00091 kg/ms to 0.00173 kg/ms at Pe = 35. However, the thermal conductivity and viscosity would

be uniform with the values of 0.628 W/mK and 0.00110 kg/ms, respectively, by neglecting the effects of particle migration throughout the tube cross section.

The higher thermal conductivity near the tube surface is achieved due to the higher concentration of the particles in this region. This fact can significantly improve the convection heat transfer. It is clear from Fig. 8 that at lower Peclet numbers, the thermal conductivity distribution becomes more uniform and consequently, the thermal conductivity would have higher values near the tube surface. On the other hand, the effect of Brownian motion on particle migration will increase compared to the other factors at low Peclet numbers. Thus, the Brownian motion makes the concentration distribution more uniform which leads to the increment of thermal conductivity near the tube surface. It can be inferred that such spatial heterogeneity in thermal conductivity distribution results in a relatively substantial modification of the thermal field, which can remarkably influence the heat transfer rate of nanofluids.

The variation of Nusselt number with Reynolds number for different nanofluid concentrations is shown in Fig. 9. It is observed that increasing the Reynolds number leads to the Nusselt number enhancement. The impact of nanofluid concentrations on the Nusselt number is more noticeable at lower Reynolds numbers due to the insignificant influence of flow momentum on heat transfer.

The convective heat transfer enhancement due to the application of SiO$_2$/water nanofluid can be obtained by the calculation of nanofluid to the base fluid Nusselt number ratio. Fig. 10 depicts the heat transfer enhancement versus Reynolds number at different concentrations. It is seen that the heat transfer performance is intensified at low Reynolds numbers. This improvement is greater at higher concentrations. A maximum of 43.9%
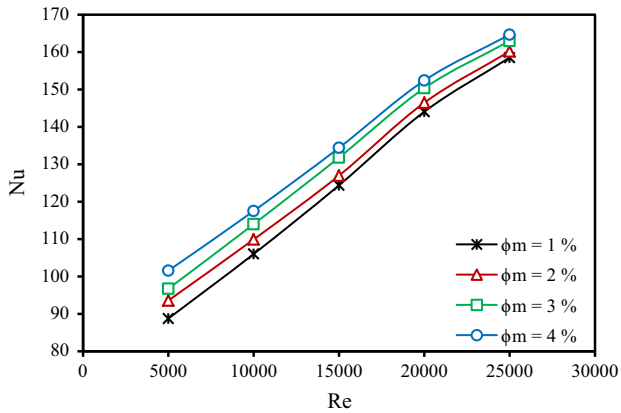
Fig. 9. Nusselt number versus Reynolds number for different mean concentrations.
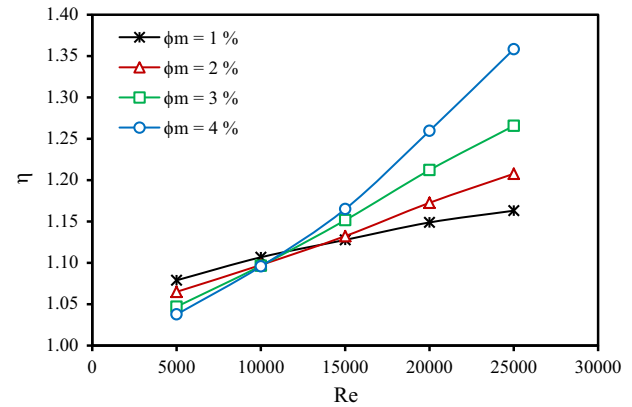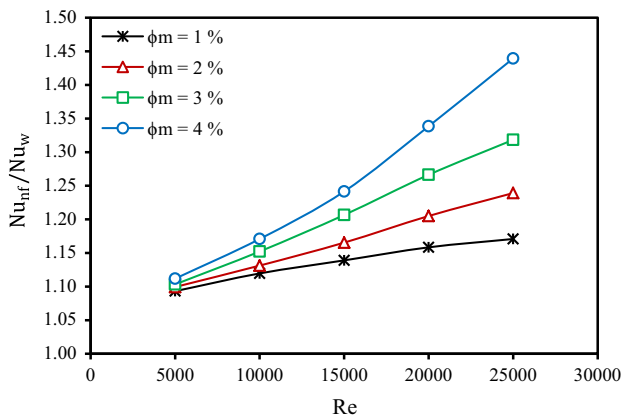

Fig. 10. Heat transfer enhancement versus Reynolds number for different mean concentrations.

enhancement in convection heat transfer is achieved by dispersion of 4% SiO₂ nanoparticles inside water at Re = 25,000.

The friction factor of SiO₂/water nanofluid is calculated and presented in Fig. 11 for different Reynolds numbers and mean concentrations. It is observed that the friction factor decreases with the increment of Reynolds number and nanoparticle mean concentration. The reason is that the viscosity of nanofluid increases by dispersion of nanoparticle into the water and also, the high velocity of the fluid at high Reynolds numbers lead to increase in friction factor.
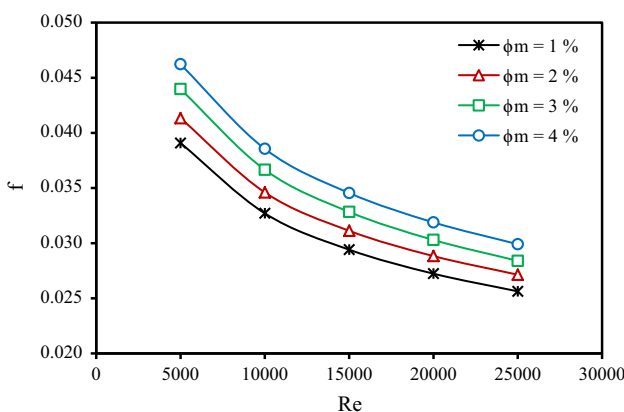
Fig. 11. Friction factor of SiO₂/water nanofluid for various mean concentrations.

Fig. 12. Influence of nanofluid concentration on the thermal performance index in different Reynolds numbers.

As seen previously, using a nanofluid in convective heat transfer processes increments the heat transfer and pressure drop, simultaneously. Regarding the evaluation of flow and heat transfer of SiO₂/water nanofluid, a hydrothermal efficiency index (η) is defined as below.

$$\eta = \frac{\frac{Nu_{nf}}{Nu_f}}{\left(\frac{f_{nf}}{f_f}\right)^{1/3}} \tag{32}$$

For better illustration, the variation of the hydrothermal efficiency index versus Reynolds number at different concentration of nanoparticles is shown in Fig. 12. It is achieved that the SiO₂/
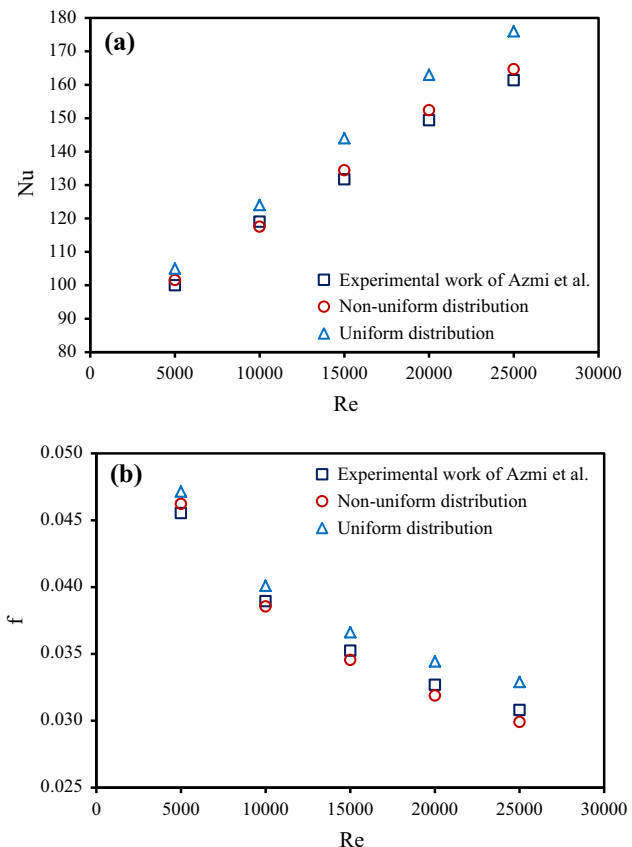

Fig. 13. Comparison of (a) Nusselt number and (b) Friction factor of experimental results and current simulations at φ_m = 4%.

water nanofluid offers higher hydrothermal efficiency index compared to the pure fluid and accordingly, the enhancement of heat transfer rate is dominant the increase of friction factor in this study. In fact, the hydrothermal efficiency index of nanofluid varies directly as concentration and Reynolds number. The highest hydrothermal efficiency is observed at $Re = 25,000$ with 4% nanoparticle concentration.

The results of the current numerical analysis are compared with the results obtained from the experimental work of Azmi et al. (2013). Fig. 13 shows the Nusselt number and friction factor obtained from current study considering homogeneous and heterogeneous concentration distribution with the experimental data at $\varphi_m = 4\%$ for different Reynolds numbers. It is revealed that the results of numerical analysis incorporating heterogeneous concentration distribution are in reasonable agreement with the experimental data, while the experimental data are overestimated by considering uniform concentration distribution. For the homogeneous concentration distribution condition, the thermal conductivity near the tube surface is higher than that of uniform condition. Meanwhile, the accuracy of the results incorporating homogeneous concentration distribution deteriorates with the increment of Reynolds number. A seen in Fig. 5, incrementing the Reynolds number causes the heterogeneity of concentration distribution. Moreover, the non-homogenous viscosity distribution causes a greater friction factor.

5. Conclusion

A numerical analysis was conducted to evaluate flow and heat transfer of SiO_2/water nanofluids in a horizontal tube for turbulent regime considering heterogeneous concentration distribution using two-phase mixture model. The concentration distribution heterogeneity enhances with the increment of Reynolds number, Peclet number, nanoparticle size and mean concentrations. This spatial heterogeneity leads to non-uniform thermophysical properties. The higher thermal conductivity near the tube surface was achieved due to the higher concentration of the particles in that region. The achieved nanoparticle distribution was implemented for analysis of nanofluid using two-phase mixture model. It was observed that incrementing Reynolds number and nanofluid mean concentration lead to the Nusselt number enhancement. The influence of nanofluid concentration on the Nusselt number was more noticeable in lower Reynolds numbers due to the insignificant influence of flow momentum on heat transfer. The maximum of 43.9% enhancement in convection heat transfer was reached by dispersion of 4% SiO_2 nanoparticles inside water at $Re = 25,000$. It was observed that the friction factor decreased with the increment of Reynolds number and nanoparticle mean concentration. The thermal performance index of the SiO_2/water nanofluid was attained greater than unity in all conditions. Therefore, heat transfer improvement overcomes the increment of friction factor in the present work. Moreover, it was revealed that the results of numerical analysis considering heterogeneous concentration distribution were in reasonable agreement with the experimental data, while the experimental data were overrated by considering homogeneous concentration distribution.

References

Amani, M., Ameri, M., Kasaeian, A., 2017a. Investigating the convection heat transfer of Fe₃O₄ nanofluid in a porous metal foam tube under constant magnetic field. Exp. Therm. Fluid Sci. 82, 439–449.

Amani, M., Ameri, M., Kasaeian, A., 2017b. The experimental study of convection heat transfer characteristics and pressure drop of magnetite nanofluid in a porous metal foam tube. Transp. Porous Media 116, 959–974.

Amani, M., Ameri, M., Kasaeian, A., 2017c. The efficacy of magnetic field on the thermal behavior of MnFe₂O₄ nanofluid as a functional fluid through an open-cell metal foam tube. J. Magn. Magn. Mater. 432, 539–547. http://dx.doi.org/10.1016/j.jmmm.2017.02.045.

Aminfar, H., Motallebzadeh, R., 2012. Investigation of the velocity field and nanoparticle concentration distribution of nanofluid using Lagrangian-Eulerian approach. J. Dispers. Sci. Technol. 33, 155–163.

Azmi, W.H., Sharma, K.V., Sarma, P.K., Mamat, R., Anuar, S., Dharma Rao, V., 2013. Experimental determination of turbulent forced convection heat transfer and friction factor with SiO₂ nanofluid. Exp. Therm. Fluid Sci. 51, 103–111.

Bahiraei, M., 2015. Studying nanoparticle distribution in nanofluids considering the effective factors on particle migration and determination of phenomenological constants by Eulerian-Lagrangian simulation. Adv. Powder Technol. 26, 802–810.

Bahiraei, M., 2016. Particle migration in nanofluids: a critical review. Int. J. Therm. Sci. 109, 90–113.

Bahiraei, M., 2017. Impact of thermophoresis on nanoparticle distribution in nanofluids. Res. Phys. 7, 136–138.

Bahiraei, M., Hosseinalipour, S.M., 2013. Particle migration in nanofluids considering thermophoresis and its effect on convective heat transfer. Thermochim. Acta 574, 47–54.

Brinkman, H.C., 1952. The viscosity of concentrated suspensions and solutions. J. Chem. Phys. 20, 571.

Buongiorno, J., 2006. Convective transport in nanofluids. J. Heat Transf. 128, 240–250.

Cai, J., Hu, X., Xiao, B., Zhou, Y., Wei, W., 2017. Recent developments on fractal-based approaches to nanofluids and nanoparticle aggregation. Int. J. Heat Mass Transf. 105, 623–637.

Chen, X., Lam, Y., Wang, Z., Tan, K., 2004. Determination of phenomenological constants of shear-induced particle migration model. Comput. Mater. Sci. 30, 223–229.

Colangelo, G., Favale, E., Miglietta, P., de Risi, A., Milanese, M., Laforgia, D., 2015. Experimental test of an innovative high concentration nanofluid solar collector. Appl. Energy 154, 874–881.

Colangelo, G., Favale, E., Miglietta, P., Milanese, M., de Risi, A., 2016a. Thermal conductivity, viscosity and stability of Al₂O₃-diathermic oil nanofluids for solar energy systems. Energy 95, 124–136.

Colangelo, G., Milanese, M., De, R., 2016b. Numerical simulation of thermal efficiency of an innovative Al₂O₃ nanofluid solar thermal collector: influence of nanoparticles concentration. Therm. Sci. 168–168.

Ding, Y., Wen, D., 2005. Particle migration in a flow of nanoparticle suspensions. Powder Technol. 149, 84–92.

Gnielinski, V., 1976. New equations for heat and mass-transfer in turbulent pipe and channel flow. Int. Chem. Eng. 16, 359–368.

Heyhat, M.M., Kowsary, F., 2010. Effect of particle migration on flow and convective heat transfer of nanofluids flowing through a circular pipe. J. Heat Transf. 132, 62401.

Iacobazzi, F., Milanese, M., Colangelo, G., Lomascolo, M., de Risi, A., 2016. An explanation of the Al₂O₃ nanofluid thermal conductivity based on the phonon theory of liquid. Energy 116, 786–794.

Kakaç, S., Pramuanjaroenkij, A., 2016a. Single-phase and two-phase treatments of convective heat transfer enhancement with nanofluids – a state-of-the-art review. Int. J. Therm. Sci. 100, 75–97.

Kakaç, S., Pramuanjaroenkij, A., 2016b. Analysis of convective heat transfer enhancement by nanofluids: single-phase and two-phase treatments. J. Eng. Phys. Thermophys. 89, 758–793.

Kasaeian, A., Eshghi, A.T., Sameti, M., 2015. A review on the applications of nanofluids in solar energy systems. Renew. Sustain. Energy Rev. 43, 584–598.

Keblinski, P., Phillpot, S., Choi, S.U., Eastman, J., 2002. Mechanisms of heat flow in suspensions of nano-sized particles (nanofluids). Int. J. Heat Mass Transf. 45, 855–863.

Keshavarz Moraveji, M., Hejazian, M., 2012. Modeling of turbulent forced convective heat transfer and friction factor in a tube for Fe₃O₄ magnetic nanofluid with computational fluid dynamics. Int. Commun. Heat Mass Transf. 39, 1293–1296.

Lam, Y.C., Chen, X., Tan, K.W., Chai, J.C., Yu, S.C.M., 2004. Numerical investigation of particle migration in poiseuille flow of composite system. Compos. Sci. Technol. 64, 1001–1010.

Launder, B.E., Spalding, D.B., 1972. Lectures in Mathematical Models of Turbulence. Academic Press.

Lomascolo, M., Colangelo, G., Milanese, M., de Risi, A., 2015. Review of heat transfer in nanofluids: conductive, convective and radiative experimental results. Renew. Sustain. Energy Rev. 43, 1182–1198.

Manninen, M., Taivassalo, V., Kallio, S., 1996. On the Mixture Model for Multiphase Flow. Technical Research Centre of Finland.

McNab, G., Meisen, A., 1973. Thermophoresis in liquids. J. Colloid Interface Sci. 44, 339–346.

Milanese, M., Iacobazzi, F., Colangelo, G., de Risi, A., 2016. An investigation of layering phenomenon at the liquid–solid interface in Cu and CuO based nanofluids. Int. J. Heat Mass Transf. 103, 564–571.

Milanese, M., Colangelo, G., Cretì, A., Lomascolo, M., Iacobazzi, F., de Risi, A., 2016a. Optical absorption measurements of oxide nanoparticles for application as nanofluid in direct absorption solar power systems – Part I: water-based nanofluids behavior. Sol. Energy Mater. Sol. Cells 147, 315–320.

Milanese, M., Colangelo, G., Cretì, A., Lomascolo, M., Iacobazzi, F., de Risi, A., 2016b. Optical absorption measurements of oxide nanoparticles for application as nanofluid in direct absorption solar power systems – Part II: ZnO, CeO₂, Fe₂O₃ nanoparticles behavior. Sol. Energy Mater. Sol. Cells 147, 321–326.

Phillips, R., Armstrong, R., Brown, R., 1992. A constitutive equation for concentrated suspensions that accounts for shear-induced particle migration. Phys. Fluids A Fluid Dyn. 4, 30–40.

Raja, M., Vijayan, R., Dineshkumar, P., Venkatesan, M., 2016. Review on nanofluids characterization, heat transfer characteristics and applications. Renew. Sustain. Energy Rev. 64, 163–173.

Russell, W.B., Schowalter, W., Saville, D., 1991. Colloidal Dispersions. Cambridge University Press.

Schiller, L., Naumann, Z., 1935. A drag coefficient correlation. Vdi Zeitung. 77, 51.

Sert, İ.O., Sezer-Uzol, N., 2016. Numerical analysis of convective heat transfer of nanofluids in circular ducts with two-phase mixture model approach. Heat Mass Transf. 52, 1841–1850.

Shariat, M., Moghari, R.M., Sajjadi, S.M., Khojamli, M., 2013. Numerical investigation of Al_2O_3/water nanofluid in horizontal elliptic ducts using two phase mixture model. J. Comput. Theor. Nanosci. 10, 199–207.

Siavashi, M., Jamali, M., 2016. Heat transfer and entropy generation analysis of turbulent flow of TiO_2-water nanofluid inside annuli with different radius ratios using two-phase mixture model. Appl. Therm. Eng. 100, 1149–1160.

Sundar, L.S., Naik, M.T., Sharma, K.V., Singh, M.K., Siva, T.C., 2012. Experimental investigation of forced convection heat transfer and friction factor in a tube with Fe_3O_4 magnetic nanofluid. Exp. Therm. Fluid Sci. 37, 65–71.

Vanaki, S.M., Ganesan, P., Mohammed, H.A., 2016. Numerical study of convective heat transfer of nanofluids: a review. Renew. Sustain. Energy Rev. 54, 1212–1239.

Wen, D., Ding, Y., 2004. Experimental investigation into convective heat transfer of nanofluids at the entrance region under laminar flow conditions. Int. J. Heat Mass Transf. 47, 5181–5188.

Wen, D., Zhang, L., He, Y., 2009. Flow and migration of nanoparticle in a single channel. Heat Mass Transf. 45, 1061–1067.

White, F., Corfield, I., 2006. Viscous Fluid Flow, vol. 3. McGraw-Hill, New York.

Xuan, Y., Li, Q., 2003. Investigation on convective heat transfer and flow features of nanofluids. J. Heat Transf. 125, 151.

Xuan, Y., Roetzel, W., 2000. Conceptions for heat transfer correlation of nanofluids. Int. J. Heat Mass Transf. 43, 3701–3707.

Yang, C., Peng, K., Nakayama, A., Qiu, T., 2016. Forced convective transport of alumina–water nanofluid in micro-channels subject to constant heat flux. Chem. Eng. Sci. 152, 311–322.

Yu, W., Choi, S., 2003. The role of interfacial layers in the enhanced thermal conductivity of nanofluids: a renovated maxwell model. J. Nanoparticle Res. 5, 167–171.